Article

Cell Reports

Brown Adipogenic Reprogramming Induced by a Small Molecule

Graphical Abstract

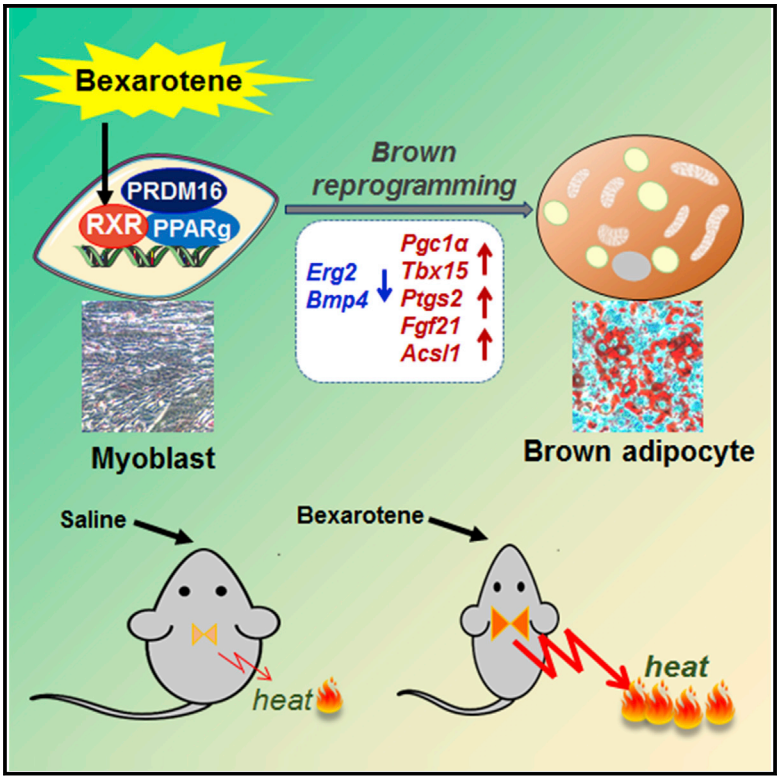

Highlights

- Bexarotene was identified as a hit to convert myoblasts into brown-like adipocytes
- Bexarotene induces brown reprogramming via RXR
- PRDM16 is required for bexarotene/RXR-induced browning
- Oral bexarotene treatment enhances BAT mass and function in mice

Authors

Baoming Nie, Tao Nie, Xiaoyan Hui, ..., Aimin Xu, Donghai Wu, Sheng Ding

Correspondence

wu_donghai@gibh.ac.cn (D.W.), sheng.ding@gladstone.ucsf.edu (S.D.)

In Brief

Employing high-throughput phenotypic screening, Nie et al. identify a retinoid X receptor agonist, bexarotene, as a hit compound that reprograms myoblasts into brown adipocytes. This reprograming requires a transcription coregulator, PRDM16, and the browning capacity of bexarotene was verified in mice. Overall, these insights point to the role of RXRs as master regulators of brown and beige fat development and activation and open a potential strategy for therapeutic manipulation of brown/beige fat function.

Accession Numbers

GSE52364

Nie et al., 2017, Cell Reports *18*, 624–635
January 17, 2017
http://dx.doi.org/10.1016/j.celrep.2016.12.062

CellPress

OPEN ACCESS
CellPress

Cell Reports
Article

Brown Adipogenic Reprogramming Induced by a Small Molecule

Baoming Nie,[1,8] Tao Nie,[2,3,4,8] Xiaoyan Hui,[5,8] Ping Gu,[6] Liufeng Mao,[3,4] Kuai Li,[3,4] Ran Yuan,[3,4] Jiashun Zheng,[7] Haixia Wang,[1] Ke Li,[1] Shibing Tang,[1] Yu Zhang,[1] Tao Xu,[1] Aimin Xu,[5] Donghai Wu,[3,4,*] and Sheng Ding[1,9,*]

[1]Gladstone Institute of Cardiovascular Disease, Department of Pharmaceutical Chemistry, University of California, San Francisco, San Francisco, CA 94158, USA
[2]Central Laboratory of the First Affiliated Hospital of Jinan University, Guangzhou 510630, China
[3]CAS Key Laboratory of Regenerative Biology, Joint School of Life Sciences, Guangzhou Medical University, Guangzhou 511436, China
[4]Guangzhou Institutes of Biomedicine and Health, Chinese Academy of Sciences, Guangzhou 510530, China
[5]State Key Laboratory of Pharmaceutical Biotechnology, The University of Hong Kong, Hong Kong, China
[6]Department of Endocrinology, School of Medicine, Nanjing University, Nanjing General Hospital of Nanjing Military Command, Nanjing 210002, China
[7]Department of Biochemistry and Biophysics, University of California, San Francisco, San Francisco, CA 94158, USA
[8]Co-first author
[9]Lead Contact
*Correspondence: wu_donghai@gibh.ac.cn (D.W.), sheng.ding@gladstone.ucsf.edu (S.D.)
http://dx.doi.org/10.1016/j.celrep.2016.12.062

SUMMARY

Brown adipose tissue (BAT) has attracted considerable research interest because of its therapeutic potential to treat obesity and associated metabolic diseases. Augmentation of brown fat mass and/or its function may represent an attractive strategy to enhance energy expenditure. Using high-throughput phenotypic screening to induce brown adipocyte reprogramming in committed myoblasts, we identified a retinoid X receptor (RXR) agonist, bexarotene (Bex), that efficiently converted myoblasts into brown adipocyte-like cells. Bex-treated mice exhibited enlarged BAT mass, enhanced BAT function, and a modest browning effect in subcutaneous white adipose tissue (WAT). Expression analysis showed that Bex initiated several "browning" pathways at an early stage during brown adipocyte reprogramming. Our findings suggest RXRs as new master regulators that control brown and beige fat development and activation, unlike the common adipogenic regulator PPARγ. Moreover, we demonstrated that selective RXR activation may potentially offer a therapeutic approach to manipulate brown/beige fat function in vivo.

INTRODUCTION

Reprogramming of one cell type into another that does not fall into the downstream differentiated lineages by defined genetic factors has attracted enormous interest for biomedical research and potential therapeutic applications. Although ex vivo reprogramming could provide desired cells for cell-based therapy, in vivo reprogramming of endogenous cells may represent an alternative and perhaps desirable strategy for modifying diseases. For example, functional β cells (Zhou et al., 2008), cardiomyocytes (Jayawardena et al., 2012; Qian et al., 2012), and neurons (Torper et al., 2013) have been generated in situ via reprogramming of endogenous relevant cell types by ectopic expression of transcription factors and microRNAs. In contrast, in vivo reprogramming by small molecules would mitigate issues associated with gene therapy.

We set out to investigate whether brown adipocyte-like cells could be generated from the non-brown adipose tissue (BAT) lineage via a small-molecule reprogramming strategy. White adipose tissue (WAT) and BAT exhibit opposite functions in whole-body energy homeostasis. Although white adipocytes function as energy storage depots, brown adipocytes are specialized in dissipating energy in the form of heat through uncoupled respiration (Cannon and Nedergaard, 2004). Brown adipocyte-like cells can be induced under different conditions and originate from different precursor cell types (Hanssen et al., 2016; Rosen and Spiegelman, 2014; Sanchez-Gurmaches et al., 2012). The classic interscapular BAT shares the same precursor with skeletal myoblasts based on transcription profile (Timmons et al., 2007). It was subsequently revealed the transcription factor *PRDM16* is a master BAT regulator and could convert skeletal myoblasts into BAT-like adipocytes (Seale et al., 2008). In contrast, brown-like adipocytes in WAT induced by β-adrenergic stimulation or cold exposure originate from a distinct lineage similar to mesenchymal precursor cells, which are much closer to white adipocytes and display a unique set of molecular signatures (Guerra et al., 1998). More recently, this type of energy-burning but genetically distinct fat cell—beige cell (or "brite" or "recruited" cell)—was characterized in mice and adult humans (Cypess et al., 2013; Lidell et al., 2013; Wu et al., 2012). Interestingly, it was reported that some beige adipocytes come from smooth muscle-like precursor cells (Long et al., 2014).

The finding that adult humans have a significant amount of BAT inversely correlated with body mass index has fueled

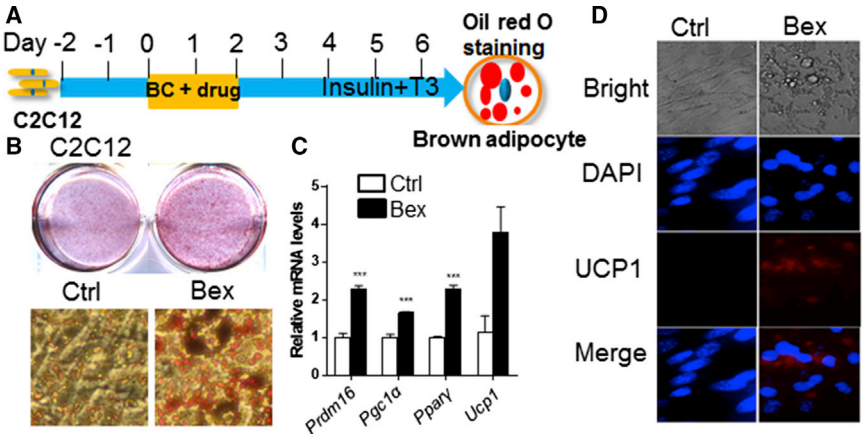

Figure 1. High-Throughput Screening Identified Bex, which Induces Brown Adipogenic Reprogramming of Committed Myoblasts

(A) Schematic of the high-throughput chemical screening for brown adipogenic reprogramming of committed myoblasts.

(B) Bex-induced BAT-like adipocytes from C2C12 myoblasts. Lipid droplets were stained by oil red O.

(C) qPCR analysis of BAT genes in BAT-like adipocytes from C2C12 myoblasts. Data were normalized to Ctrl and represented mean ± SEM. $^{**}p < 0.01$, $^{***}p < 0.001$ (n = 3).

(D) UCP1 immunostaining in Bex-induced BAT-like adipocytes from C2C12 myoblasts.

considerable interest in the therapeutic potential of brown adipocytes (Cypess et al., 2009; van Marken Lichtenbelt et al., 2009; Virtanen et al., 2009). A small amount of BAT (*i.e.*, 50 g) was estimated to be sufficient to increase a person's energy metabolism by 20%, which would be equivalent to a reduction of body weight by 4–20 kg over 1 year (Rosen and Spiegelman, 2014; Tseng et al., 2010). Activation of BAT was reported to reduce elevated triglyceride concentrations and alleviate obesity in humans (Bartelt et al., 2011). Furthermore, BAT transplantation efficiently decreased body weight and improved glucose homeostasis and insulin sensitivity in both chow- and high-fat diet (HFD)-fed mice (Liu et al., 2013; Min et al., 2016; Stanford et al., 2013). Consequently, a better understanding and improved ability to pharmacologically control BAT identity and function may provide a new therapeutic strategy for the treatment of obesity and related disorders.

Unlike genetic manipulation, which may cause mutations, induction of BAT mass/activity by small molecules likely represents a safer approach to benefit overall metabolism. To this end, we carried out high-throughput phenotypic screening for induced brown adipocyte reprogramming in committed myoblasts and identified bexarotene (hereafter referred to as Bex), a specific retinoid X receptor (RXR) agonist (Boehm et al., 1995), as a potent and specific small molecule for reprogramming of myoblasts into brown adipocyte-like cells. Bex selectively induced BAT identity/features in multiple cell types while inhibiting WAT differentiation. Bex-treated mice had more BAT mass, enhanced metabolic function, and constrained body weight gain compared with control mice. Further mechanistic studies established RXRα and RXRγ as new master regulators of BAT development that act upstream of PRDM16 and other browning genes to instate BAT identity.

RESULTS

Bex Selectively Promotes Brown Adipogenesis but Inhibits White Adipogenesis

To identify small molecules that mimic overexpression of PRDM16 to induce brown adipocyte reprogramming in non-brown pre-adipocyte cells, high-throughput phenotypic screening of 20,000 compounds was performed in committed skeletal myoblasts (C2C12 cells) for brown adipogenic induction with oil red O staining as a readout (Figure 1A). Under basal conditions (BCs), no adipocyte-like cells could be induced from C2C12 myoblasts. In contrast, several hit compounds, including Bex, could induce adipogenesis in C2C12 cells. Given the previous finding that RXR has a role in UCP1 induction in brown adipocytes (Alvarez et al., 2000), we focused our studies on examining whether and how Bex/RXR could induce brown adipocyte reprogramming in non-brown pre-adipocyte cells. Further experiments confirmed that treatment with Bex (10 μM) for 2 days potently initiated adipogenic reprogramming in C2C12 cells (Figure 1B). Interestingly, although peroxisome proliferator-activated receptor γ (PPARγ) agonists (rosiglitazone/Rosig) typically exhibiting browning effects could enhance brown adipocyte reprogramming induced by Bex, rosiglitazone itself could not induce any adipogenic phenotype in C2C12 myoblasts (Figure S1A), suggesting that Bex is a more powerful browning inducer.

Gene expression analysis showed that Bex also induced *Pparγ* expression and brown adipocyte-specific genes, including *Prdm16*, *Pgc1α*, and *Ucp1* (Figure 1C). Immunofluorescence staining confirmed that UCP1 protein was significantly induced by Bex in reprogrammed adipocytes from C2C12 cells (Figure 1D). To further establish the specificity of brown reprogramming induced by Bex, we also examined the effects of Bex and an RXR antagonist (HX531) on white pre-adipocytes and brown pre-adipocytes. Remarkably, Bex inhibited white adipogenic differentiation in white pre-adipocytes (3T3-L1) and mesenchymal precursor cells (C3H10T1/2) under strong adipogenic induction conditions; HX531 promoted white adipogenic differentiation from both cell types (Figure S1B). In contrast, Bex promoted brown adipogenic differentiation in pre-adipocyte cells, and HX531 inhibited both basal and Bex-induced brown adipogenic differentiation in pre-BAT cells (Figure S1B). These results collectively suggest that Bex (and RXR agonism) exhibit a specific brown adipocyte-like reprogramming effect.

Bex Induces Brown Adipogenic Reprogramming via Activation of RXRα and RXRγ

Bex was originally developed as a selective RXR agonist without RXR subtype specificity (Boehm et al., 1995). To further characterize the mechanism by which Bex induces brown adipogenic

reprogramming, we first examined whether RXR and its subtypes (Mangelsdorf et al., 1992) were required for Bex function. It was found that selective RXR antagonist HX531 or knockdown of *Rxrs* by specific short hairpin RNAs (shRNAs) targeting *Rxrα*, *Rxrβ* and *Rxrγ* individually could almost completely abolish Bex-induced brown adipogenic reprogramming in C2C12 myoblasts (Figures 2A and 2B; Figure S2A). These results established that the effect of Bex is dependent on RXR agonism.

To further characterize the role of RXR subtypes, *Rxrα*, *β*, and *γ* were individually overexpressed in C2C12 cells. *Rxrα*, *β*, or *γ* overexpression alone was not sufficient to induce adipogenic reprogramming in C2C12 cells. However, treatment with Bex for 2 days in conjunction with *Rxrα* or *Rxrγ* overexpression induced nearly all cells into brown adipocyte-like cells with multilocular lipid droplets (Figure 2C; Figure S2B), although Bex treatment with *Rxrβ* overexpression only slightly increased efficiency of brown adipogenic reprogramming (Figure 2C). Gene expression analysis demonstrated that these reprogrammed cells expressed typical BAT genes at levels comparable with those in differentiated brown adipocytes, including the general adipogenic genes *Pparγ* and *adiponectin* (Figure 2D), and BAT-specific genes, including *Ucp1*, *Prdm16*, *Pparα*, *Pparδ*, *Cox7a1*, and *Cox8b* (Figure 2E). Consistently, immunofluorescence staining against UCP1 confirmed its significant protein induction in those reprogrammed cells (Figure 2F). On the other hand, myogenic genes, including *Myf5*, *MyoD*, and *MyoG*, and the late myogenic marker *Mhcβ* were dramatically downregulated in these cells (Figure S2C). Furthermore, similar brown adipogenic induction was observed in primary committed myoblasts that were treated with Bex and *Rxr* overexpression (Figure 2G; Figure S2D), indicating that the effect of Bex is not cell line-dependent. We found that various types of WAT cells all express much higher levels of *Rxrβ* than *Rxrα* and *Rxrγ*. Interestingly, BAT and skeletal muscle express a similar level of *Rxrβ* as WAT but much higher levels of *Rxrα* and *Rxrγ* than WATs (Figure 2H). Moreover, robust brown adipogenic induction could also be achieved in mesenchymal precursor cells that were treated with Bex and *RXR* overexpression (Figure S2E). Consistently, Bex/RXRα and Bex/RXRγ suppressed WAT-specific genes, such as *resistin* (*Retn*), *resistin-like alpha* (*retnlα*), and *phosphoserine aminotransferase 1* (*Psat1*) (Figure S2F), in C3H10T1/2 cells undergoing adipogenic induction, whereas they induced BAT-characteristic small multilocular lipid droplets (Figure S2E) and BAT-specific genes, including *Ucp1*, *Prdm16*, *Pparα*, *Pgc1α*, *Cox7a1*, and *Cox8b* (Figure S2G). Bex alone can induce UCP1 protein in C3H10T1/2 cells (Figure S2H). Taken together, these results suggest that *Rxrα/γ* activation is required and sufficient for brown adipogenic induction in committed myoblasts and mesenchymal precursor cells that normally do not commit toward the brown adipogenic lineage.

Bex and RXR-Mediated Brown Adipogenic Induction Is Partially Dependent on PRDM16

PRDM16 was previously shown to be a master brown adipogenic regulator, and its overexpression can induce browning in C2C12 myoblasts. To delineate the RXR mechanism in relation to PRDM16 in brown adipogenic induction, we first examined the gene expression changes of *Prdm16* during the Bex/RXR-induced brown adipogenic reprogramming process. Interestingly, Bex induced *Prdm16* expression and dramatically induced *Ucp1* in *RXRα*-overexpressed C2C12 cells at an early stage before exhibiting typical adipogenic phenotypes (Figure 3A). Both *Rxrα* and *Rxrγ* significantly induced *Prdm16* and *Ucp1* expression after Bex stimulation for 2 days, but *Rxrβ* only increased *Ucp1* expression. However, overexpression of *Pparγ2* itself or plus rosiglitazone did not induce *Prdm16* and *Ucp1* expression (Figure 3B). This result indicates that Bex-RXRα/γ may act upstream of *Prdm16*. Interestingly, knockdown of *Prdm16* by shRNA only partially decreased Bex and Bex/RXR-induced brown adipogenic reprogramming of C2C12 cells (Figure 3C) (the efficiency of *Prdm16* knockdown in pre-brown adipocyte is approximately 70%; Figure S3A), suggesting that additional RXR downstream effectors mediate brown adipogenic induction. Consistently, Bex was shown to potentiate *Prdm16* overexpression-induced *Ucp1* expression 4-fold in primary committed myoblasts (Figure 3D). Furthermore, Bex treatment of *Prdm16*-overexpressing myoblasts generated brown adipocyte-like cells with much smaller lipid droplets (i.e., more BAT-like) than those in cells with *Prdm16* overexpression alone (Figure 3D), suggesting that the downstream mechanism of Bex/RXR is not solely dependent on PRDM16. It was previously shown that neither *Prdm16* overexpression in white pre-adipocytes nor *Prdm16* knockdown in brown pre-adipocytes under adipogenic induction could affect the adipogenesis phenotype (Seale et al., 2007). In contrast, RXR agonism acts upstream of *Prdm16* and clearly functions as a more powerful master regulator on inducing brown adipogenic phenotypes.

To further confirm the role of *Prdm16* in the Bex/RXR-induced brown adipogenic process, we used clustered regularly interspaced short palindromic repeats (CRISPR)/Cas9 gene-editing technique to completely knock out *Prdm16* in C3H10T1/2 cells (Figure S3B). In *Prdm16* knockout cells, Bex-induced *Ucp1*, *Cox7a1*, and *Pparα* expression was significantly but incompletely abolished (Figure 3E). Knockout of *Prdm16* had no significant effect on the expression of *Fabp4* (also known as *aP2*), suggesting that it has no key role in adipogenesis. However, *Pgc1α* was completely abolished by *Prdm16* knockout (Figure 3E). These results suggest that brown adipocyte reprogramming induced by Bex/RXR is not completely dependent on *Prdm16*.

Bex Initiates "Browning" Pathways at an Early Stage of Adipogenesis in C2C12 Cells

To further dissect the transcriptional mechanism downstream of Bex/RXR, we performed transcriptome analysis of Bex treatment at the early stage of brown adipogenic reprogramming in C2C12 cells (i.e., 2 days of Bex treatment) using a microarray (Figure 4A). Gene ontology (GO) functional analysis revealed that the genes upregulated by Bex were significantly enriched in lipid biogenesis and brown fat cell specification (Figure 4B; cutoff of Benjamini value is < 0.01). Interestingly, there was no significant GO function enrichment in genes downregulated genes (Figure S4). To identify the minimal non-redundant set of pathways involved in this process, these changed genes were further analyzed by GO-Elite and visualized by Cytoscape (Shannon et al., 2003). Most pathways induced by Bex were implicated in adipocyte development, including adipogenesis, the PPAR

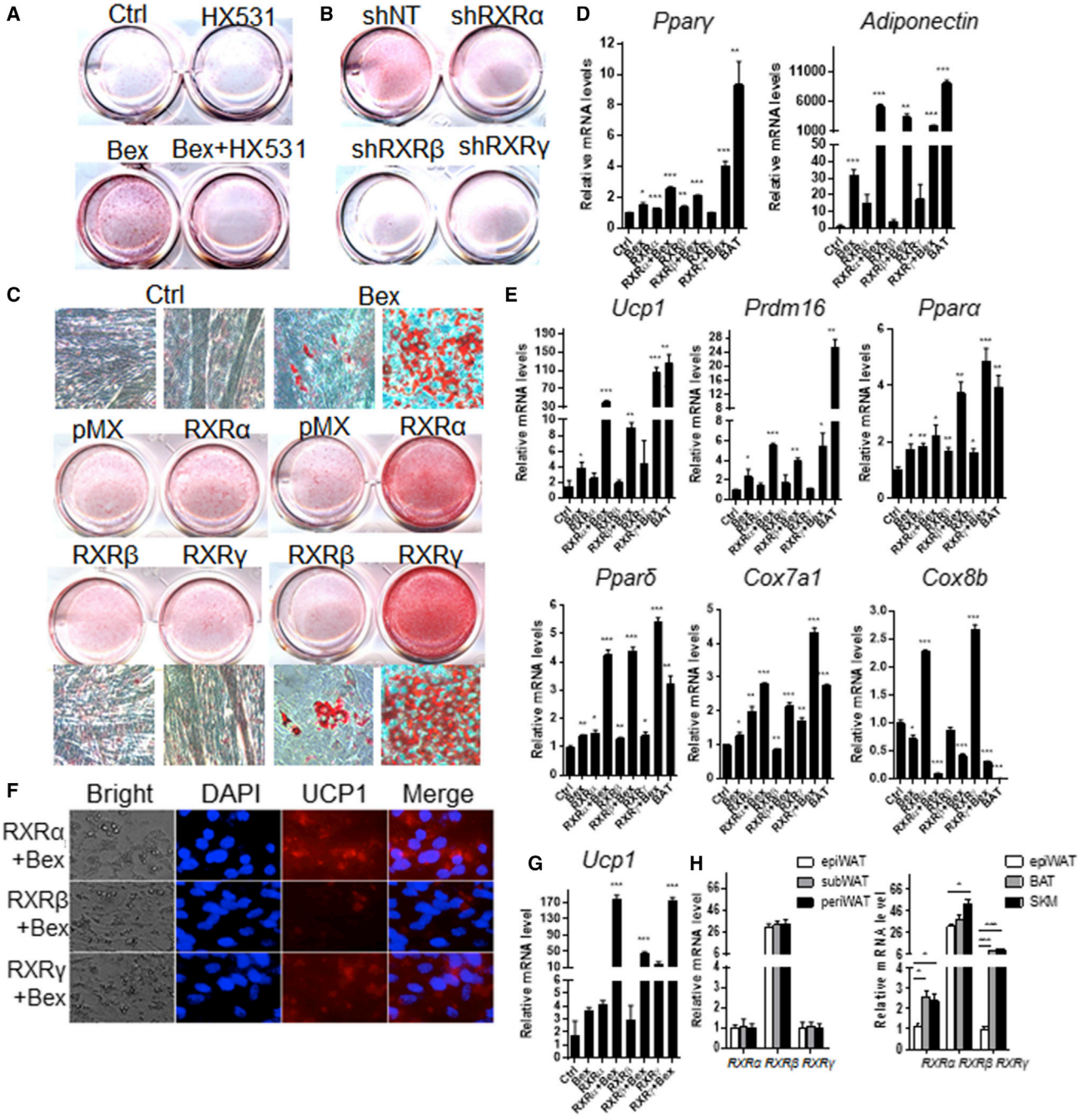

Figure 2. RXRα/γ Agonism Mediates Bex-Induced Brown Adipogenic Reprogramming

(A) The RXR antagonist HX531 inhibits Bex-induced brown adipogenic reprogramming of myoblasts.

(B) Knockdown of *Rxr* subtypes by shRNAs targeting *Rxrα*, *Rxrβ*, or *Rxrγ* abolished Bex-induced brown adipogenic reprogramming of myoblasts.

(C) Overexpression of *Rxrα* and *Rxrγ*, but not *Rxrβ*, dramatically potentiated Bex-induced brown adipogenic reprogramming of myoblasts.

(D and E) qPCR analysis of general adipogenic genes (D) and brown adipogenic genes (E) in reprogrammed cells induced by Bex treatment, RXRα/β/γ overexpression of each subtype, or combined treatment (n = 3).

(F) UCP1 immunostaining in reprogrammed brown adipogenic cells induced by Bex treatment and RXR overexpression.

(G) *Ucp1* expression in reprogrammed cells from primary myoblasts induced by Bex treatment, RXRα/β/γ subtype overexpression, or combined treatment (n = 3). Data were normalized to Ctrl and represent mean ± SEM. *p < 0.05, **p < 0.01, ***p < 0.001.

(H) RXRα, RXRβ, and RXRγ mRNA levels in WATs, BAT, and skeletal muscle (SKM). mRNA was purified in WATs, BAT, and SKM from mice (n = 5). Values are normalized to the RXRα level in epiWAT and expressed as mean ± SEM. *p < 0.05, ***p < 0.001.

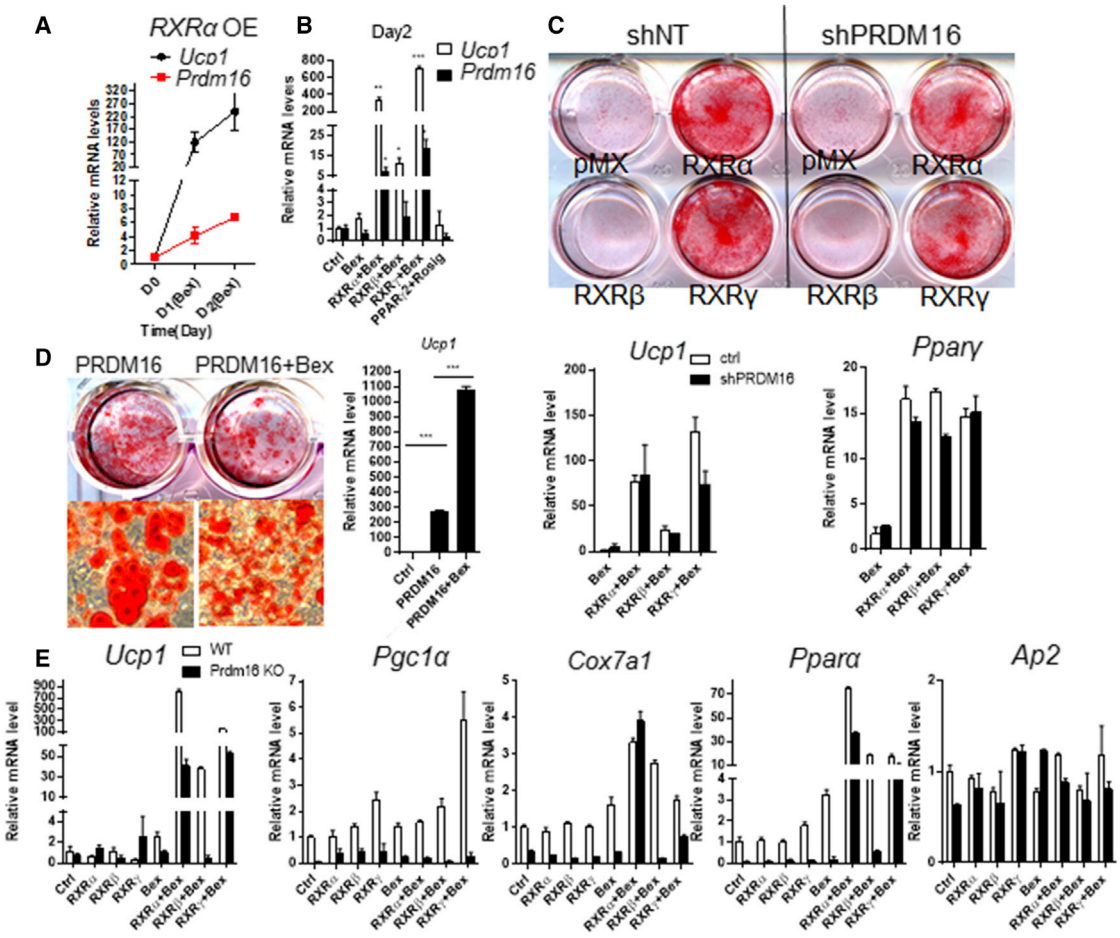

Figure 3. Bex and RXR-Mediated Brown Adipogenic Reprogramming Is Only Partially Dependent on PRDM16

(A) Induction of *Prdm16*and *Ucp1* expression by treatment with Bex and RXRα overexpression in myoblasts for the first several days.

(B) *Ucp1* and *Prdm16* levels in Bex/RXR-treated C2C12 cells on day 2. Data were normalized to Ctrl and represent mean ± SEM. *$p < 0.05$, **$p < 0.01$, ***$p < 0.001$.

(C) Knockdown of *Prdm16* only partially reduced Bex/RXR-induced brown adipogenic reprogramming of myoblasts. Ucp1 and PPARγ were examined on day 6 (n = 3).

(D) Bex and *Prdm16* synergistically induced UCP1 expression in primary myoblasts. Data were normalized to Ctrl and represented mean ± SEM. ***$p < 0.001$ (n = 3).

(E) Knockout of *Prdm16* in C3H10T1/2 cells partially reduced the expression of *Ucp1*, *Cox7a1*, and *Pparα* and completely abolished *Pgc1α* expression but did not affect *ap2* expression. Data were normalized to Ctrl and represent mean ± SEM (n = 3).

pathway, synthesis of triacylglyceride, the statin pathway, retinol metabolism, fatty acid biogenesis pathways, cholesterol biosynthesis, and mitochondrial long-chain fatty acid β-oxidation (Figure 4C).

By qPCR confirmation, Bex significantly increased expression of the general adipogenesis genes, including *Pparγ*, *Fabp4*, and *CD36*, and some downstream targets of RXR/PPARγ (e.g., *Pex11a*, *Angptl4*, and *HK2*) (Nielsen et al., 2008). In addition, Bex treatment increased the expression of genes with a known browning effect, such as *Fgf21*, *Pgc1α*, *Acsl1*, *Tbx15*, *Ptgs2*, and *G0S2* (Figure 4D). *Fgf21* has a physiological role in thermogenesis of WATs. *Fgf21* knockout mice displayed an impaired ability to adapt to chronic cold exposure with diminished browning of WAT (Fisher et al., 2012). *Pgc1α* is a key regulator of mitochondrial biogenesis and function and is essential for BAT function (Lin et al., 2004; Ventura-Clapier et al., 2008). *Acsl1* is responsible for mitochondrial long-chain fatty acid β-oxidation and required for cold thermogenesis (Ellis et al., 2010). *Tbx15* is essential for brown and beige, but not white, adipocyte differentiation (Gburcik et al., 2012). Moreover, white adipogenic differentiation of 3T3-L1 pre-adipocytes was impaired by *Tbx15* overexpression (Gesta et al., 2011). Overexpression of *Ptgs2* (also known as *Cox-2*) in WAT induced de novo browning recruitment in WAT, increased systemic energy expenditure, and protected mice against high-fat diet-induced obesity (Madsen et al., 2010; Vegiopoulos et al., 2010). *G0S2* (G0/G1 switch gene 2) expression was also induced, and its expression negatively correlates with the development of obesity (Yang et al., 2010). On the other hand, Bex repressed some white adipogenesis-associated genes, such as *Bmp4* and *Egr2* (also known as

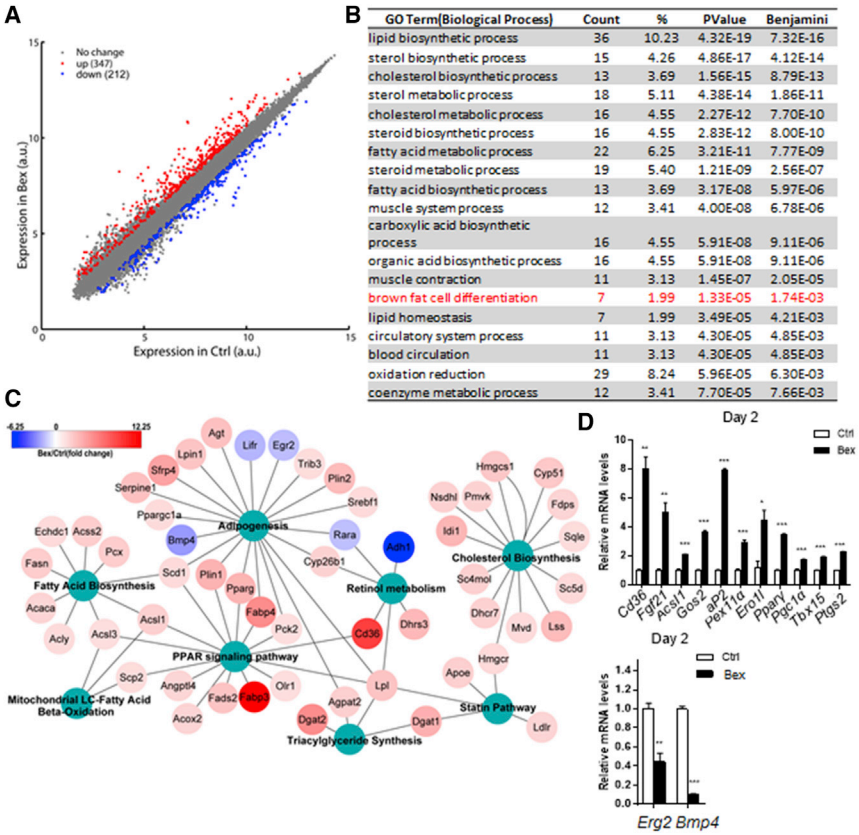

GO Term(Biological Process)	Count	%	PValue	Benjamini
lipid biosynthetic process	36	10.23	4.32E-19	7.32E-16
sterol biosynthetic process	15	4.26	4.86E-17	4.12E-14
cholesterol biosynthetic process	13	3.69	1.56E-15	8.79E-13
sterol metabolic process	18	5.11	4.38E-14	1.86E-11
cholesterol metabolic process	16	4.55	2.27E-12	7.70E-10
steroid biosynthetic process	16	4.55	2.83E-12	8.00E-10
fatty acid metabolic process	22	6.25	3.21E-11	7.77E-09
steroid metabolic process	19	5.40	1.21E-09	2.56E-07
fatty acid biosynthetic process	13	3.69	3.17E-08	5.97E-06
muscle system process	12	3.41	4.00E-08	6.78E-06
carboxylic acid biosynthetic process	16	4.55	5.91E-08	9.11E-06
organic acid biosynthetic process	16	4.55	5.91E-08	9.11E-06
muscle contraction	11	3.13	1.45E-07	2.05E-05
brown fat cell differentiation	7	1.99	1.33E-05	1.74E-03
lipid homeostasis	7	1.99	3.49E-05	4.21E-03
circulatory system process	11	3.13	4.30E-05	4.85E-03
blood circulation	11	3.13	4.30E-05	4.85E-03
oxidation reduction	29	8.24	5.96E-05	6.30E-03
coenzyme metabolic process	12	3.41	7.70E-05	7.66E-03

Figure 4. Bex Initiates Browning Pathways at an Early Stage of Brown Adipogenic Reprogramming of Myoblasts

(A) Scatterplot of differentially expressed genes in Ctrl and Bex-treated samples on day 2. Genes upregulated by Bex are marked in red, and those downregulated are shown in blue.

(B) DAVID GO analysis of upregulated genes induced by Bex treatment.

(C) Enriched molecular pathways of differentially expressed genes in GO-Elite.

(D) Real-time PCR confirmed mRNA levels of some adipogenesis and browning genes induced by Bex in C2C12 cells on day 2. Data were normalized to Ctrl and represent mean ± SEM. *$p < 0.05$, **$p < 0.01$, ***$p < 0.001$ ($n = 3$).

krox20) (Figure 4D). *Bmp4* specifically promotes white adipogenic differentiation of C3H10T1/2 cells and even lowers the *Ucp1* level in brown pre-adipocytes (Boehm et al., 1995; Tseng et al., 2008). The transcription factor *Egr2* was reported to be essential for 3T3-L1 differentiation via activation of the transcriptional activator of *C/EBPβ*. Conversely, knockdown of *Egr2* inhibited white adipogenic differentiation of 3T3-L1 cells (Chen et al., 2005). These data provide a map of the molecular pathway for brown adipogenic induction in C2C12 cells, and support Bex/RXR as a master regulator of BAT/beige specification by modulating a spectrum of adipogenic pathways with a specificity of inducing brown-selective genes while suppressing white-selective genes.

Bex Increases BAT Mass and Function In Vivo

Given the specific and remarkable brown adipogenic activity of Bex in vitro and the existence of relevant cell types in vivo, we next examined whether this reprogramming activity would have any corresponding effect in mice. Bex at 50 mg/kg/day was orally administered to mice for 4 weeks along with a high-fat diet. Despite similar food intake (Figure S5A), Bex-treated mice displayed less gain of body weight (Figure 5A) than control mice, suggesting that Bex likely increases energy expenditure in mice. To test this possibility, we carried out indirect calorimetry with these mice. Bex-treated mice consumed more oxygen (Figure 5B) and expended significantly more total energy, as quantified by heat generation, than the saline-treated group (Figure 5C) without change in physical activity (Figure S5B). Consistent with this result, mice treated with Bex showed a higher rectal temperature than control mice when challenged with 6°C temperature (Figure 5D), which suggests that Bex-treated mice are more cold tolerant. In addition, to examine whether Bex influences the sympathetic drive, oxygen consumption in response to CL316,243 (1 mg/kg, intraperitoneal [i.p.] injection) was compared between control and Bex-treated mice. Bex-treated mice showed much higher O_2 consumption than control mice upon administration of CL316,243 (Figures S5C and S5D). These data indicate that Bex boosts energy expenditure in vivo. Furthermore, the Bex-treated mice showed improved sensitivity to glucose and insulin challenge (Figure 5E).

Body composition analysis showed that Bex-treated mice had less fat mass than control mice (Figure 5F). The masses of various fat depots were also examined at the end of the experiment. Interscapular BAT mass (in both the absolute tissue weight and its proportion to body weight) was increased significantly in Bex-treated mice compared with control mice (Figures 5G and 5H). Furthermore, qPCR analysis showed a striking augmentation of thermogenic gene expression in BAT from Bex-treated mice compared with control mice, including increased *Ucp1*, *Pgc1α*, *Prdm16*, *Pparα*, *Pparγ*, and *Pparδ* levels (Figure 5I). A significant browning effect in subcutaneous/inguinal WAT (subWAT) was also demonstrated because *Ucp1*, *Pgc1α*, *Prdm16*, *Pparα*, and *Pparδ* were dramatically induced, and *Pparγ* was repressed. However, there was no significant change in epididymal WAT (epiWAT) and retroperitoneal WAT (periWAT) (Figure 5I). Consistent with microarray data in vitro, some browning-related genes, such as *Fgf21*, *Tbx15*, and *Ptgs2*, were increased, but *Egr2* and *Bmp4* were repressed, by Bex in BAT. Only *Fgf21* was significantly increased, and *Egr2* was repressed in subWAT (Figure 5I). UCP1 immunostaining showed more UCP1 signal in BAT and subWAT (Figure 5J). Furthermore, H&E staining showed much smaller lipid droplets in BAT and subWAT from Bex-treated

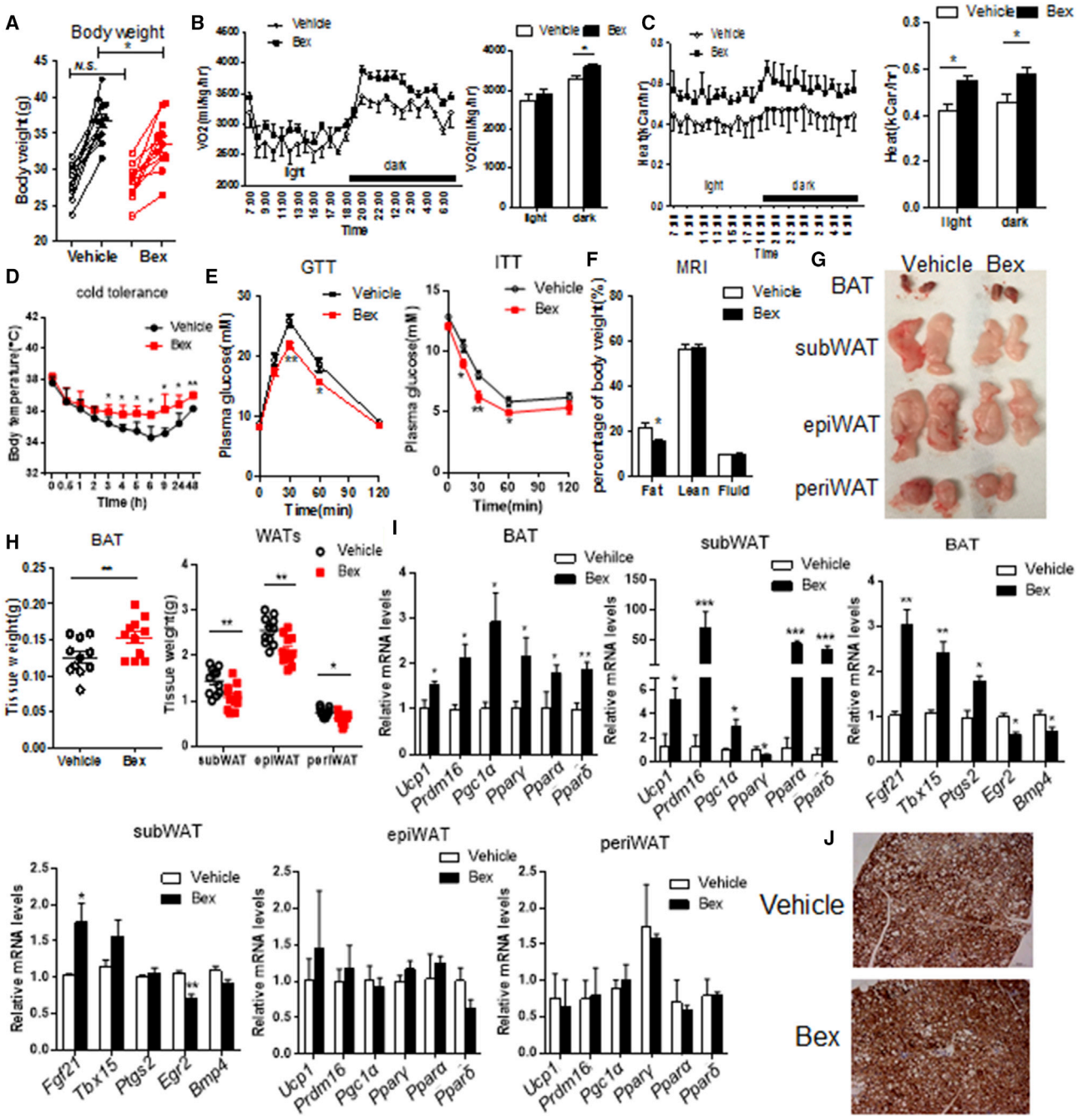

Figure 5. Bex Increases BAT Mass and Function In Vivo

(A) Bex treatment significantly reduced body weight gain in mice (n = 9). *p < 0.05; N.S., no significance.

(B) Bex treatment increased oxygen consumption (VO_2) in mice (n = 9). *p < 0.05.

(C) Bex treatment increased heat release in mice (n = 9). *p < 0.05.

(D) Bex treatment promoted cold tolerance (n = 9). *p < 0.05.

(E) Bex increased the glucose tolerance test (GTT) and insulin tolerance test (ITT) response in mice (n = 9). *p < 0.05.

(F) A positron emission tomography (PET) scan showed body composition in mice (n = 9). *p < 0.05.

(G and H) Bex treatment increased BAT mass but decreased WAT mass in mice. Representative fat images (G) and quantification of different kinds of fat mass (H) (n = 9). *p < 0.05.

(I) qPCR analysis of BAT genes in BAT, subWAT, epiWAT, and periWAT in control and Bex-treated mice (n = 9). Data were normalized to the vehicle group and represented mean ± SEM. *p < 0.05, **p < 0.01.

(J) UCP1 immunostaining in BAT.

mice than from control mice, suggesting that the enlarged BAT mass was due to increased brown adipocyte cell number (Figure S5E). H&E staining and gene expression showed that Bex had no significant effect on skeletal muscle (Figure S5F) and liver (Figure S5G). To check whether Bex had a direct thermogenic induction effect in mature adipocytes, we tested the effect of Bex in mature adipocytes differentiated from primary precursors. Stimulation of Bex for 24 hr induced Ucp1 expression in mature BAT and subWAT but not in epiWAT (Figure S5H). Taken together, these results demonstrate that Bex exhibits a browning effect in BAT and subWAT against HFD-induced phenotypes in mice.

DISCUSSION

The rising prevalence of metabolic diseases such as obesity and diabetes has become a major public health concern. Recently, brown fat biology has been gaining interest because BAT mediated thermogenesis was proposed as a mechanism to treat obesity and insulin resistance. From high-throughput phenotypic screening, we identified that the specific RXR agonist Bex has the capacity to induce reprogramming of committed myoblasts into BAT-like adipocytes. Our studies revealed that Bex/RXR have opposing roles in WAT versus BAT induction in vitro. In a panel of cell types, including committed myoblast cells, white pre-adipocytes, mesenchymal precursor cells, and brown pre-adipocytes, Bex inhibited white adipogenesis and induced brown adipogenic specification, suggesting that it specifically endows brown adipogenic phenotypes to relevant cells. In vivo data also showed that Bex enhances metabolism by increasing BAT mass/function and inducing a browning effect in subWAT.

Interestingly, a recent study revealed that adipocyte-specific *Prdm16* knockout mice using an *adiponectin*-Cre do not exhibit different interscapular BAT mass and function than wild-type mice (Cohen et al., 2014), suggesting that PRDM16 plays a critical role during development to orchestrate BAT rather than to execute BAT functionality. Indeed, PRDM16 was found to be essential for beige cell induction, where new sets of browning arsenals need to be implemented. However, another report found that PRDM16 is dispensable for embryonic BAT development because lineage ablation of *Prdm16* using a *myf5*-Cre leaves BAT more or less intact, whereas it causes upregulation of white fat cell-selective genes in adult mice (Harms et al., 2014). These studies hint that other transcription factors, in addition to PRDM16, may play a more deterministic role during classic BAT development. This expression profile of RXRs appears to correlate with the determinant role of *Rxr*α and *Rxr*γ rather than *Rxr*β in BAT specification. This may also indicate that selective regulation of *Rxr* subtypes might provide specificity to target specific cell types for modulating metabolism.

The nuclear receptor PPARγ has been regarded as a "master" regulator of fat cell development and function. More recently, it was revealed that certain PPARγ agonists, such as rosiglitazone, have browning effects in WAT, possibly by stabilizing the PRDM16 protein level (Ohno et al., 2012). Our expression analysis also demonstrated that PPAR pathways were induced by Bex/RXR. Interestingly, in contrast to the ability of Bex to induce brown adipogenic reprogramming of C2C12 cells, our data and other published results show that rosiglitazone could not induce adipogenic specification in myoblast cells (Seale et al., 2008). Furthermore, although *Ppar*γ overexpression could drive adipogenesis, it does not induce the brown adipogenic gene program in myoblast cells (Seale et al., 2008). This suggests that Bex/RXR acts upstream of the PPAR pathway and that it has additional downstream effectors to initiate the browning process. Indeed, we found that PRDM16, the master regulator of BAT development, is also induced by Bex/RXR. It has been shown that PPARγ and PRDM16 form a complex to regulate downstream browning cascades (Seale et al., 2008). A recent study revealed that EBF2 is another BAT determinant. In addition, RXRα potentiates the binding of EBF2-PPARγ on the *Prdm16* promoter and, thus, directly activates *Prdm16* transcription (Rajakumari et al., 2013). It is now recognized that PPARγ has a common and distinct binding pattern in different WATs and BAT to define adipocyte types (Rajakumari et al., 2013; Siersbæk et al., 2012). RXR might be a druggable target to change the PPARγ chromatin binding pattern to activate browning genes while repressing WAT programs.

UCP1 plays a key role in the thermogenic regulation of body weight. Increased content of UCP1 in adipose tissue is strongly linked to protection against diet-induced obesity. Our in vivo data demonstrated efficient induction of *Ucp1* and other thermogenic genes by Bex, with higher metabolic activity and less weight gain. More interestingly, Bex increased BAT mass significantly, probably by promoting de novo BAT induction from progenitor cells because the BAT mass was not due to enlargement of brown adipocytes. These data revealed a dual function of the RXR pathway: regulating BAT function and controlling BAT mass. Furthermore, there is also a significant increase in UCP1 in subWAT from Bex-treated mice than from control mice but not in epiWAT. However, it is difficult to quantify the thermogenesis contribution of increased BAT mass and direct thermogenesis induction in mature BAT and subWAT. In line with the augmented expression of *Ucp1* in Bex-treated mice, these mice exhibited enhanced cold tolerance in the cold challenge and higher O_2 consumption upon acute CL316,243 stimulation. However, it should be noted that, in a cold tolerance experiment, the metabolic energy output is contributed from both non-shivering thermogenesis of BAT and shivering thermogenesis of skeletal muscles, whereas measuring the response to sympathetic nervous system activation in awake animals tends to show higher inter-animal variability (Cannon and Nedergaard, 2011). Thus, norepinephrine injection in anesthetized mice warrants future investigation to evaluate the effect of Bex on the thermogenic capacity of BAT.

In conclusion, our data revealed that Bex/RXR functions as a master regulator to control *Ppar*γ and *Prdm16* expression and other downstream pathways with a browning effect, including *Fgf21*, *Pgc1*α, and *Tbx15*. Our studies shed new light on the retinoid pathway in BAT/beige specification and function and demonstrate that energy metabolism can be enhanced by a small molecule via increasing BAT mass and function. Many unanswered questions remain, relating to how RXRs precisely control adipogenic subtype specification in development, tissue

homeostasis, and disease, that would warrant subsequent studies.

EXPERIMENTAL PROCEDURES

Cell Culture

C2C12, 3T3-L1, and C3H10T1/2 cells were purchased from the ATCC. Immortalized brown pre-adipocytes were kindly donated by Prof. C. Ronald Kahn (Harvard University). Primary myoblasts were purified from mouse limb muscles and cultured in growth medium (F10 + 20% fetal bovine serum [FBS] + 5 ng/mL basic fibroblast growth factor [bFGF]) in Matrigel-coated plates. Adipocyte differentiation was induced by treating cells for 2 days under basal adipogenesis conditions (850 nM insulin, 1 nM T3, 0.5 mM isobuylmethylxanthine, 125 μM indomethacin, and 5 μM dexamethasone in 10% FBS DMEM) (Seale et al., 2008). Then cells were switched to 10% FBS DMEM containing 850 nM insulin and 1 nM T3 only for another 4–6 days. To stimulate thermogenesis, cells were stimulated with 10 μM forskolin for 4 hr.

Adipogenesis Screening in C2C12 Cells

C2C12 cells were plated at 3,000 cells/well onto 384-well plates using a liquid distributor (BioTek Instruments Elx405). When cells reached confluency, the medium was changed to basal adipogenesis medium, and compounds were delivered from a chemical library using the Biomek FX^P 2000 machine (a laboratory automation workstation). After 2 days of incubation, the medium was changed to 10% FBS DMEM containing 850 nM insulin and 1 nM T3 only for another 4 days, and then the cells were fixed and stained for oil red O. We screened about 20,000 chemicals from the NIH library, Sigma LOPAC1280 library, ENZO fatty acid library (BML-2803), Bioactive lipid library (BML-2800), and S.D. lab in-house libraries.

Preparation of Mouse Primary Myoblasts Derived from Satellite Cells

Primary myoblasts were purified from 4-week-old C57BL/6J mice as described previously (Xiao et al., 2011). The limb muscles were dissected out and rinsed in ice-cold PBS. The muscles were cut into fine pieces using scissors, and the minced tissue was vigorously mixed and spun at 1,300 rpm for 4 min. The minced tissue pellet was then resuspended in 10 mL DMEM and 1 mL of 1% pronase (to a final concentration of 0.1%) and incubated at 37°C with continuous shaking for 1.5 hr before being spun down at 1,300 rpm for 5 min. The pellet was resuspended in 5∼10 mL DMEM and triturated 15-20 times to loosen cells before being filtered through a 100-μm cell strainer. The flow-through was collected, spun down, and resuspended in 10 mL of growth medium (F10 + 20% FBS + 5 ng/mL bFGF) in non-coated plates to allow fibroblasts to attach for 60 min. The floating cells were transferred to a plate coated with Matrigel (BD Biosciences), and the growth medium was changed every 36 hr.

Constructs and Chemicals

The mouse RXRα and RXRγ plasmids were from Dr. Ronald Evans (Salk Institute), and the mouse RXRβ plasmid was purchased from OriGene. These three RXR fragments were subcloned into the pMXs retrovirus construct (Yamanaka lab, Gladstone Institutes) via the EcoRI site. All constructs were sequenced for verification. Non-target shRNA(shNT), shRXRα, shRXRβ, and shRXRγ lentivirus constructs were purchased from Sigma-Aldrich. Retrovirus PRDM16 (plasmid 15504) and PRDM16 shRNA (plasmid 15505) constructs were purchased from Addgene. Retrovirus and lentivirus constructs were packaged in Plat E and 293T cells, respectively. Bexarotene, HX531, and rosiglitazone were purchased from Thermo Fisher Scientific, Tocris Bioscience, and Sigma-Aldrich, respectively.

Real-Time PCR

Total RNA from cell lines was purified using a QIAGEN kit, and total RNA from mouse tissues was extracted using Trizol. RNA concentration and quality were measured by a NanoDrop spectrometer. Complementary DNA was prepared from total RNA with the iScriptIII DNA synthesis kit (Bio-Rad). Quantitative PCR reactions containing SYBR-Green fluorescent dye were performed using the ABI7900HT (Applied Biosystems) following the manufacturer's protocols. Relative mRNA expression was determined by the ΔΔ-Ct method with *Gapdh* as an endogenous control. Primer sequences are shown in Table S1.

Immunofluorescence

After induction of adipogenesis in C2C12 cells and C3H10T1/2 cells with or without Bex, cells were fixed with formaldehyde for 10 min, then washed with PBS and penetrated with 0.1% Triton X-100. Samples were incubated in blocking buffer containing 3% BSA for 1 hr at room temperature. Samples were then incubated with ab23841 at a 1:200 dilution for 1 hr in BSA/Tris-buffered saline (TBS). Cells were incubated with Alexa Fluor 555 secondary antibody (Invitrogen) for 1 hr at room temperature, and nuclei were stained with DAPI (Sigma-Aldrich). Images were acquired by a Zeiss Axioimager Z1 equipped with an Apotome system and processed using Zeiss Axiovision software.

Affymetrix Microarray Analysis

Total RNA samples were purified from C2C12 cells after 2-day basal adipogenesis medium treatment without or with Bex (control [Ctrl] and Bex) with the RNeasy mini plus kit from QIAGEN. Microarray analyses were performed in duplicate from independent biologic samples according to the standard Affymetrix Genechip protocol. Purified RNA was analyzed for quality using chip-based capillary electrophoresis (Bioanalyzer, Agilent), and quantity and purity were determined with a NanoDrop spectrometer. NuGEN Pico V2, based on Ribo single prime isothermal amplification (Ribo-SPIA) technology, was used for amplification, fragmentation, and biotin labeling. The labeled cDNA was hybridized to mouse Gene 1.0 sense target (ST) microarrays (Affymetrix). The signal intensity fluorescent images produced during Affymetrix gene chip hybridizations were read using the Affymetrix Model 3000 scanner and converted into GeneChip probe results files (Command and Expression Console software [CEL]) using Command and Expression Console software (Affymetrix). Data were normalized and analyzed using Affymetrix Expression Console and Transcriptome Analysis Console (TAC) software. Arrays were normalized for array-specific effects using Affymetrix Robust Multi-Array (RMA) normalization. A gene was regarded as significantly changed when the p value was <0.05 and fold was >1.5 or <−1.5. Results were deposited in GEO: GSE52364.The differential expression gene list was further analyzed in The Database for Annotation, Visualization and Integrated Discovery (DAVID) GO functional annotation and GO-Elite (Zambon et al., 2012).

CRISPR/Cas9 Gene Editing

We designed two pairs of guide RNAs (gRNAs) targeting Exon3 of mouse *Prdm16*:gRNA1:95-gcccagctctacgagggcctagg-118, gRNA2(RC):155-gctgcc cacgccaaggccctcgg-132. We subcloned gRNA into the LentiCRISPR lentiviral CRISPR/Cas9 construct (Addgene). *Prdm16* gRNA F1: 5′-CAC CGg ccc agc tct acg agg gcct-3′; *Prdm16* gRNA R1: AAA Cag gcc ctc gta gag ctg ggcC-3′; *Prdm16* gRNA F2: 5′-CAC CGg ctg ccc acg cca agg ccct-3′; *Prdm16* gRNA R2: 5′-AAA Cag ggc ctt ggc gtg ggc agcC-3′. We followed the Lenti CRISPR Lentiviral CRISPR/Cas9 and Single Guide RNA Guide. Virus particles were packaged in 293T cells. C3H10T1/2 cells were infected with the virus from gRNA1 or gRNA2 and then selected with 1 μg/mL puromycin for two passages before single-cell dilution. Single cells were expanded enough for the following experiments. We amplified the fragment using this pair of PCR primers: forward, 5′-GAA GGA AGC TGG TTA GGA GTA G-3′; reverse, 3′-GGA CCA GGA CCT TTA TGG TAA G-5′. The amplicon was checked by PCR, and the candidates were subcloned into TA-clone and then sequenced to verify the frameshift knockout cell line. Our data showed that only gRNA2 works that can generate the *Prdm16* frameshift mutation.

Animal Work

C57BL/6J mice were fed, ad libitum, a standard laboratory chow diet (LabDiet 5053, LabDiet). Animals were housed under 12-hr light-dark cycles with a controlled temperature (23°C ± 1°C). The body weight of 8-week-old male mice (n = 14) was measured and randomly divided into two groups (n = 7

in each group). The mice were treated with Bex (50 mg/kg/day) or saline by daily oral gavage for 4 weeks and fed with an HFD (21.9 kJ/g, 60% of energy from fat, 20% of energy from protein, 20% of energy from carbohydrates; D12492; Research Diet). The food intake and body weight were monitored. Minispec time domain magnetic resonance equipment (TD-NMR) analyzers (Bruker Instruments) were used to evaluate body composition on anesthetized animals. One day prior to the cold challenge, the holding cages were prechilled at 6°C overnight. The next day, the mice were acutely shifted from 22°C to 6°C with two mice in each cage. The rectal temperature was examined by 4610 Precision Thermometer (Measurement Specialty) at various time points. Alternatively, the mice were acclimated in Comprehensive Lab Animal Monitoring System (CLAMS) for 3 days before CL316,243 (1 mg/kg body weight) was intraperitoneally injected. The oxygen consumption was recorded for 3 hr afterward. When all functional assays were finished, the mice were sacrificed, fat tissues were collected, and tissue mass was measured. All collected tissues were stored in a −80°C degree freezer or liquid nitrogen for further experiments. All animal experiments were conducted in accordance with the institutional guidelines for humane treatment of laboratory animals of the University of Hong Kong (HKU) Animal Care and Use Committee and University of California, San Francisco's Institutional Animal Care and Use Committee.

Indirect Calorimetry

Whole-body O_2 consumption, CO_2 production, heat generation, food intake, and physical activity were measured using an open circuit indirect calorimetry system with automatic temperature and light controls (Columbus Instruments). Mice had access ad libitum to chow and water in respiration chambers, and data were recorded for a 48-hr period before acclimatization for 24 hr.

Isolation and Differentiation of Adipocytes and Stromal Vascular Cells from Adipose Tissues

Brown, inguinal, or epididymal adipose tissues were dissected from C57BL/6J mice, rinsed in phosphate-buffered saline, minced, and digested for 40 min at 37°C in 0.1% (w/v) type I collagenase solution (Sigma) in D-Hank's buffer. The digested tissue was filtered through a 250-μm nylon mesh and centrifuged at 800 × *g* for 3 min. The sediment was resuspended in DMEM (Gibco) with 10% fetal bovine serum (HyClone). Two days after reaching confluence (day 0), the cells were induced to differentiate into adipocytes in medium containing 5 μg/ml insulin (Sigma), 1 μM dexamethasone (Sigma), 0.5 mM isobutylmethylxanthine (Calbiochem), and 1 μM rosiglitazone (Sigma). Two days later, the medium was replaced with DMEM supplemented with 10% fetal bovine serum, 5 μg/ml insulin, and 1 μM rosiglitazone, and the cells were cultured for 6 days. The mature adipocytes were stimulated by Bex for 24 hr, and then Ucp1 mRNA levels were examined by qPCR.

Histochemistry

Epididymal, inguinal, and retroperitoneal white and brown adipose tissues were fixed in 4% formaldehyde overnight at room temperature immediately after sacrifice. Tissues were paraffinized and sectioned by microtome, and the slides were stained with H&E (Sigma) following the standard protocol. Sections were examined by light microscopy. Photomicrographs were scanned using an Abaton Scan 300/Color scanner.

Statistical Analysis

Unless otherwise stated, data are presented as the mean ± SEM, and significant differences were analyzed by two-tailed Student's t tests. O_2 consumption, CO_2 production, and heat generation data were analyzed by analysis of covariance (ANCOVA), with body weight as covariant in accordance with a recent publication (Himms-Hagen et al., 2000).

ACCESSION NUMBERS

The accession number for the microarray gene expression data reported in this paper is GEO: GSE52364 (http://www.ncbi.nlm.nih.gov/geo/query/acc.cgi?token=azgpcsashxaxbur&acc=GSE52364).

SUPPLEMENTAL INFORMATION

Supplemental Information includes five figures and one table and can be found with this article online at http://dx.doi.org/10.1016/j.celrep.2016.12.062.

AUTHOR CONTRIBUTIONS

B.N., D.W., and S.D. conceived and designed the experiments. B.N., T.N., X.H., P.G., L.M., and R.Y. performed the experiments. J.Z. assisted with the microarray data analysis. H.W., Kuai Li, Ke Li, Y.Z., T.X., and S.T. contributed reagents/materials. B.N., A.X., D.W., and S.D. wrote the paper.

ACKNOWLEDGMENTS

We are grateful for technical assistance from the Gladstone Genomics Core and thank Robert V. Farese, Jr. and Gary Howard at Gladstone Institutes for editorial assistance. We also appreciate the efforts of the Jianhua Shao lab in pilot mouse work at UCSD. S.D. is supported by funding from NICHD, NHLBI, NEI/NIH, California Institute for Regenerative Medicine, and the Gladstone Institutes. This work was supported in part by funds from the National Basic Research Program of China (2016YFC1305000 and 2010CB945500), a key international collaborative fund from the Chinese Academy of Sciences (154144KYSB20150019), Natural Science Foundation of Guangdong Province (2016A030310122), and Science and Technology Planning Project of Guangdong Province (2011A060901019).

Received: May 6, 2016
Revised: August 18, 2016
Accepted: December 20, 2016
Published: January 17, 2017

REFERENCES

Alvarez, R., Checa, M., Brun, S., Viñas, O., Mampel, T., Iglesias, R., Giralt, M., and Villarroya, F. (2000). Both retinoic-acid-receptor- and retinoid-X-receptor-dependent signalling pathways mediate the induction of the brown-adipose-tissue-uncoupling-protein-1 gene by retinoids. Biochem. J. *345*, 91–97.

Bartelt, A., Bruns, O.T., Reimer, R., Hohenberg, H., Ittrich, H., Peldschus, K., Kaul, M.G., Tromsdorf, U.I., Weller, H., Waurisch, C., et al. (2011). Brown adipose tissue activity controls triglyceride clearance. Nat. Med. *17*, 200–205.

Boehm, M.F., Zhang, L., Zhi, L., McClurg, M.R., Berger, E., Wagoner, M., Mais, D.E., Suto, C.M., Davies, J.A., Heyman, R.A., et al. (1995). Design and synthesis of potent retinoid X receptor selective ligands that induce apoptosis in leukemia cells. J. Med. Chem. *38*, 3146–3155.

Cannon, B., and Nedergaard, J. (2004). Brown adipose tissue: function and physiological significance. Physiol. Rev. *84*, 277–359.

Cannon, B., and Nedergaard, J. (2011). Nonshivering thermogenesis and its adequate measurement in metabolic studies. J. Exp. Biol. *214*, 242–253.

Chen, Z., Torrens, J.I., Anand, A., Spiegelman, B.M., and Friedman, J.M. (2005). Krox20 stimulates adipogenesis via C/EBPbeta-dependent and -independent mechanisms. Cell Metab. *1*, 93–106.

Cohen, P., Levy, J.D., Zhang, Y., Frontini, A., Kolodin, D.P., Svensson, K.J., Lo, J.C., Zeng, X., Ye, L., Khandekar, M.J., et al. (2014). Ablation of PRDM16 and beige adipose causes metabolic dysfunction and a subcutaneous to visceral fat switch. Cell *156*, 304–316.

Cypess, A.M., Lehman, S., Williams, G., Tal, I., Rodman, D., Goldfine, A.B., Kuo, F.C., Palmer, E.L., Tseng, Y.H., Doria, A., et al. (2009). Identification and importance of brown adipose tissue in adult humans. N. Engl. J. Med. *360*, 1509–1517.

Cypess, A.M., White, A.P., Vernochet, C., Schulz, T.J., Xue, R., Sass, C.A., Huang, T.L., Roberts-Toler, C., Weiner, L.S., Sze, C., et al. (2013). Anatomical localization, gene expression profiling and functional characterization of adult human neck brown fat. Nat. Med. *19*, 635–639.

Ellis, J.M., Li, L.O., Wu, P.C., Koves, T.R., Ilkayeva, O., Stevens, R.D., Watkins, S.M., Muoio, D.M., and Coleman, R.A. (2010). Adipose acyl-CoA synthetase-1

directs fatty acids toward beta-oxidation and is required for cold thermogenesis. Cell Metab. *12*, 53–64.

Fisher, F.M., Kleiner, S., Douris, N., Fox, E.C., Mepani, R.J., Verdeguer, F., Wu, J., Kharitonenkov, A., Flier, J.S., Maratos-Flier, E., and Spiegelman, B.M. (2012). FGF21 regulates PGC-1α and browning of white adipose tissues in adaptive thermogenesis. Genes Dev. *26*, 271–281.

Gburcik, V., Cawthorn, W.P., Nedergaard, J., Timmons, J.A., and Cannon, B. (2012). An essential role for Tbx15 in the differentiation of brown and "brite" but not white adipocytes. Am. J. Physiol. Endocrinol. Metab. *303*, E1053–E1060.

Gesta, S., Bezy, O., Mori, M.A., Macotela, Y., Lee, K.Y., and Kahn, C.R. (2011). Mesodermal developmental gene Tbx15 impairs adipocyte differentiation and mitochondrial respiration. Proc. Natl. Acad. Sci. USA *108*, 2771–2776.

Guerra, C., Koza, R.A., Yamashita, H., Walsh, K., and Kozak, L.P. (1998). Emergence of brown adipocytes in white fat in mice is under genetic control. Effects on body weight and adiposity. J. Clin. Invest. *102*, 412–420.

Hanssen, M.J., van der Lans, A.A., Brans, B., Hoeks, J., Jardon, K.M., Schaart, G., Mottaghy, F.M., Schrauwen, P., and van Marken Lichtenbelt, W.D. (2016). Short-term cold acclimation recruits brown adipose tissue in obese humans. Diabetes *65*, 1179–1189.

Harms, M.J., Ishibashi, J., Wang, W., Lim, H.W., Goyama, S., Sato, T., Kurokawa, M., Won, K.J., and Seale, P. (2014). Prdm16 is required for the maintenance of brown adipocyte identity and function in adult mice. Cell Metab. *19*, 593–604.

Himms-Hagen, J., Melnyk, A., Zingaretti, M.C., Ceresi, E., Barbatelli, G., and Cinti, S. (2000). Multilocular fat cells in WAT of CL-316243-treated rats derive directly from white adipocytes. Am. J. Physiol. Cell Physiol. *279*, C670–C681.

Jayawardena, T.M., Egemnazarov, B., Finch, E.A., Zhang, L., Payne, J.A., Pandya, K., Zhang, Z., Rosenberg, P., Mirotsou, M., and Dzau, V.J. (2012). MicroRNA-mediated in vitro and in vivo direct reprogramming of cardiac fibroblasts to cardiomyocytes. Circ. Res. *110*, 1465–1473.

Lidell, M.E., Betz, M.J., Dahlqvist Leinhard, O., Heglind, M., Elander, L., Slawik, M., Mussack, T., Nilsson, D., Romu, T., Nuutila, P., et al. (2013). Evidence for two types of brown adipose tissue in humans. Nat. Med. *19*, 631–634.

Lin, J., Wu, P.H., Tarr, P.T., Lindenberg, K.S., St-Pierre, J., Zhang, C.Y., Mootha, V.K., Jäger, S., Vianna, C.R., Reznick, R.M., et al. (2004). Defects in adaptive energy metabolism with CNS-linked hyperactivity in PGC-1alpha null mice. Cell *119*, 121–135.

Liu, X., Zheng, Z., Zhu, X., Meng, M., Li, L., Shen, Y., Chi, Q., Wang, D., Zhang, Z., Li, C., et al. (2013). Brown adipose tissue transplantation improves whole-body energy metabolism. Cell Res. *23*, 851–854.

Long, J.Z., Svensson, K.J., Tsai, L., Zeng, X., Roh, H.C., Kong, X., Rao, R.R., Lou, J., Lokurkar, I., Baur, W., et al. (2014). A smooth muscle-like origin for beige adipocytes. Cell Metab. *19*, 810–820.

Madsen, L., Pedersen, L.M., Lillefosse, H.H., Fjaere, E., Bronstad, I., Hao, Q., Petersen, R.K., Hallenborg, P., Ma, T., De Matteis, R., et al. (2010). UCP1 induction during recruitment of brown adipocytes in white adipose tissue is dependent on cyclooxygenase activity. PLoS ONE *5*, e11391.

Mangelsdorf, D.J., Borgmeyer, U., Heyman, R.A., Zhou, J.Y., Ong, E.S., Oro, A.E., Kakizuka, A., and Evans, R.M. (1992). Characterization of three RXR genes that mediate the action of 9-cis retinoic acid. Genes Dev. *6*, 329–344.

Min, S.Y., Kady, J., Nam, M., Rojas-Rodriguez, R., Berkenwald, A., Kim, J.H., Noh, H.L., Kim, J.K., Cooper, M.P., Fitzgibbons, T., et al. (2016). Human 'brite/beige' adipocytes develop from capillary networks, and their implantation improves metabolic homeostasis in mice. Nat. Med. *22*, 312–318.

Nielsen, R., Pedersen, T.A., Hagenbeek, D., Moulos, P., Siersbaek, R., Megens, E., Denissov, S., Børgesen, M., Francoijs, K.J., Mandrup, S., and Stunnenberg, H.G. (2008). Genome-wide profiling of PPARgamma:RXR and RNA polymerase II occupancy reveals temporal activation of distinct metabolic pathways and changes in RXR dimer composition during adipogenesis. Genes Dev. *22*, 2953–2967.

Ohno, H., Shinoda, K., Spiegelman, B.M., and Kajimura, S. (2012). PPARγ agonists induce a white-to-brown fat conversion through stabilization of PRDM16 protein. Cell Metab. *15*, 395–404.

Qian, L., Huang, Y., Spencer, C.I., Foley, A., Vedantham, V., Liu, L., Conway, S.J., Fu, J.D., and Srivastava, D. (2012). In vivo reprogramming of murine cardiac fibroblasts into induced cardiomyocytes. Nature *485*, 593–598.

Rajakumari, S., Wu, J., Ishibashi, J., Lim, H.W., Giang, A.H., Won, K.J., Reed, R.R., and Seale, P. (2013). EBF2 determines and maintains brown adipocyte identity. Cell Metab. *17*, 562–574.

Rosen, E.D., and Spiegelman, B.M. (2014). What we talk about when we talk about fat. Cell *156*, 20–44.

Sanchez-Gurmaches, J., Hung, C.M., Sparks, C.A., Tang, Y., Li, H., and Guertin, D.A. (2012). PTEN loss in the Myf5 lineage redistributes body fat and reveals subsets of white adipocytes that arise from Myf5 precursors. Cell Metab. *16*, 348–362.

Seale, P., Kajimura, S., Yang, W., Chin, S., Rohas, L.M., Uldry, M., Tavernier, G., Langin, D., and Spiegelman, B.M. (2007). Transcriptional control of brown fat determination by PRDM16. Cell Metab. *6*, 38–54.

Seale, P., Bjork, B., Yang, W., Kajimura, S., Chin, S., Kuang, S., Scimè, A., Devarakonda, S., Conroe, H.M., Erdjument-Bromage, H., et al. (2008). PRDM16 controls a brown fat/skeletal muscle switch. Nature *454*, 961–967.

Shannon, P., Markiel, A., Ozier, O., Baliga, N.S., Wang, J.T., Ramage, D., Amin, N., Schwikowski, B., and Ideker, T. (2003). Cytoscape: a software environment for integrated models of biomolecular interaction networks. Genome Res. *13*, 2498–2504.

Siersbæk, M.S., Loft, A., Aagaard, M.M., Nielsen, R., Schmidt, S.F., Petrovic, N., Nedergaard, J., and Mandrup, S. (2012). Genome-wide profiling of peroxisome proliferator-activated receptor γ in primary epididymal, inguinal, and brown adipocytes reveals depot-selective binding correlated with gene expression. Mol. Cell. Biol. *32*, 3452–3463.

Stanford, K.I., Middelbeek, R.J., Townsend, K.L., An, D., Nygaard, E.B., Hitchcox, K.M., Markan, K.R., Nakano, K., Hirshman, M.F., Tseng, Y.H., and Goodyear, L.J. (2013). Brown adipose tissue regulates glucose homeostasis and insulin sensitivity. J. Clin. Invest. *123*, 215–223.

Timmons, J.A., Wennmalm, K., Larsson, O., Walden, T.B., Lassmann, T., Petrovic, N., Hamilton, D.L., Gimeno, R.E., Wahlestedt, C., Baar, K., et al. (2007). Myogenic gene expression signature establishes that brown and white adipocytes originate from distinct cell lineages. Proc. Natl. Acad. Sci. USA *104*, 4401–4406.

Torper, O., Pfisterer, U., Wolf, D.A., Pereira, M., Lau, S., Jakobsson, J., Björklund, A., Grealish, S., and Parmar, M. (2013). Generation of induced neurons via direct conversion in vivo. Proc. Natl. Acad. Sci. USA *110*, 7038–7043.

Tseng, Y.H., Kokkotou, E., Schulz, T.J., Huang, T.L., Winnay, J.N., Taniguchi, C.M., Tran, T.T., Suzuki, R., Espinoza, D.O., Yamamoto, Y., et al. (2008). New role of bone morphogenetic protein 7 in brown adipogenesis and energy expenditure. Nature *454*, 1000–1004.

Tseng, Y.H., Cypess, A.M., and Kahn, C.R. (2010). Cellular bioenergetics as a target for obesity therapy. Nat. Rev. Drug Discov. *9*, 465–482.

van Marken Lichtenbelt, W.D., Vanhommerig, J.W., Smulders, N.M., Drossaerts, J.M., Kemerink, G.J., Bouvy, N.D., Schrauwen, P., and Teule, G.J. (2009). Cold-activated brown adipose tissue in healthy men. N. Engl. J. Med. *360*, 1500–1508.

Vegiopoulos, A., Müller-Decker, K., Strzoda, D., Schmitt, I., Chichelnitskiy, E., Ostertag, A., Berriel Diaz, M., Rozman, J., Hrabe de Angelis, M., Nüsing, R.M., et al. (2010). Cyclooxygenase-2 controls energy homeostasis in mice by de novo recruitment of brown adipocytes. Science *328*, 1158–1161.

Ventura-Clapier, R., Garnier, A., and Veksler, V. (2008). Transcriptional control of mitochondrial biogenesis: the central role of PGC-1alpha. Cardiovasc. Res. *79*, 208–217.

Virtanen, K.A., Lidell, M.E., Orava, J., Heglind, M., Westergren, R., Niemi, T., Taittonen, M., Laine, J., Savisto, N.J., Enerbäck, S., and Nuutila, P. (2009). Functional brown adipose tissue in healthy adults. N. Engl. J. Med. *360*, 1518–1525.

Wu, J., Boström, P., Sparks, L.M., Ye, L., Choi, J.H., Giang, A.H., Khandekar, M., Virtanen, K.A., Nuutila, P., Schaart, G., et al. (2012). Beige adipocytes are a distinct type of thermogenic fat cell in mouse and human. Cell *150*, 366–376.

Xiao, F., Wang, H., Fu, X., Li, Y., Ma, K., Sun, L., Gao, X., and Wu, Z. (2011). Oncostatin M inhibits myoblast differentiation and regulates muscle regeneration. Cell Res. *21*, 350–364.

Yang, X., Lu, X., Lombès, M., Rha, G.B., Chi, Y.I., Guerin, T.M., Smart, E.J., and Liu, J. (2010). The G(0)/G(1) switch gene 2 regulates adipose lipolysis through association with adipose triglyceride lipase. Cell Metab. *11*, 194–205.

Zambon, A.C., Gaj, S., Ho, I., Hanspers, K., Vranizan, K., Evelo, C.T., Conklin, B.R., Pico, A.R., and Salomonis, N. (2012). GO-Elite: a flexible solution for pathway and ontology over-representation. Bioinformatics *28*, 2209–2210.

Zhou, Q., Brown, J., Kanarek, A., Rajagopal, J., and Melton, D.A. (2008). In vivo reprogramming of adult pancreatic exocrine cells to beta-cells. Nature *455*, 627–632.